Functionally Graded Alumina/Mullite Coatings for Protection of Silicon Carbide Ceramic Components from Corrosion

Semiannual Report

March 1998–August 1998

Prepared by:

Prof. Stratis V. Sotirchos

October 1998

Work Performed under Grant No.: DE-FG22-96PC96208

Performed for:

U.S. Dept. of Energy
University Coal Research Program
Pittsburgh Energy Technology Center
Pittsburgh, Pennsylvania

Performed at:

University of Rochester
Dept. of Chemical Engineering
Rochester, NY 14627

EXECUTIVE SUMMARY

The main objective of this research project is the formulation of processes that can be used to prepare compositionally graded alumina/mullite coatings for protection from corrosion of silicon carbide components (monolithic or composite) used or proposed to be used in coal utilization systems (e.g., combustion chamber liners, heat exchanger tubes, particulate removal filters, and turbine components) and other energy-related applications. Mullite will be employed as the inner (base) layer and the composition of the film will be continuously changed to a layer of pure alumina, which will function as the actual protective coating of the component. Chemical vapor deposition reactions of silica, alumina, and aluminosilicates (mullite) through hydrolysis of aluminum and silicon chlorides in the presence of CO_2 and H_2 will be employed to deposit compositionally graded films of mullite and alumina. Our studies will include the kinetic investigation of the silica, alumina, and aluminosilicate deposition processes, characterization of the composition, microstructure, surface morphology, and mechanical behavior of the prepared films, and modeling of the various deposition processes.

During this six-month reporting period, the experimental work on the investigation of the deposition of alumina, silica, and aluminosilicates from mixtures of methyltrichlorosilane (MTS), aluminum trichloride, carbon dioxide, and hydrogen was continued. Experiments were also conducted on the deposition processes of the simple oxides, alumina and silica, from mixtures containing only one chloride ($AlCl_3$ and MTS, respectively). Deposition rate data were obtained in a relatively broad range of operating conditions: temperatures in the range 800-1000^oC, 100 Torr pressure, 0.006-0.015 $AlCl_3$ feed mole fraction, 0.011-0.027 CH_3SiCl_3 feed mole fraction, and 0.004-0.07 CO_2 feed mole fraction, and various positions along the axis of the deposition reactor. Since the effect of temperature had been examined in detail in the previous reporting period, our efforts were mainly concentrated on the investigation of the effects of the other parameters on the three deposition processes. The results showed that the mole fraction of CO_2 had a strong influence on all deposition rates, with the alumina deposition rate and the codeposition rate showing a tendency to increase significantly with increasing concentration of CO_2 in the feed at low mole fraction values and reach a limiting value at high CO_2/chloride ratios. The increase in the concentration of carbon dioxide had, in general, a negative effect on the rate of silica deposition. These effects were in agreement with the conclusions reached from the thermodynamic equilibrium analysis of the deposition processes in past studies. The increase in the mole fraction of $AlCl_3$ had a positive effect on the rate of codeposition and the deposition of alumina. In the case of alumina deposition, the deposition rate leveled off in some cases as the $AlCl_3$ concentration was increased, and this behavior was consistent with the results of past experimental studies. The deposition rate and the deposit stoichiometry were influenced strongly by the substrate position in the reactor, and the deposition rate could increase or decrease with increasing distance from the entrance of the reactor depending on the reaction temperature.

TABLE OF CONTENTS

EXECUTIVE SUMMARY ii

TABLE OF CONTENTS iii

LIST OF FIGURES iv

1. BACKGROUND INFORMATION 1

2. WORK DONE AND DISCUSSION 5

3. SUMMARY 11

BIBLIOGRAPHY 12

LIST OF FIGURES

Figure 1. Effect of CO_2 mole fraction on the deposition and codeposition rates at 950°C. 14

Figure 2. Effect of CO_2 mole fraction on the deposition and codeposition rates at 1000°C.. 15

Figure 3. Effect of $AlCl_3$ mole fraction on the deposition rate in the presence or absence of MTS at 950°C and 1000°C. Solid lines: codeposition; dashed lines: deposition from $AlCl_3$. 16

Figure 4. Effect of MTS mole fraction on the rate of SiO_2 deposition at 950 °C. 17

Figure 5. SEM micrographs of CVD films. Temperature = 1000°C, pressure = 100 Torr, $x_{CO2} = 0.036$, total flow rate = 250 cm^3/min, and position = 4 cm. a) silica, $x_{MTS} = 0.011$; b) alumina, $x_{AlCl3} = 0.009$. 18

Figure 6. SEM micrographs of codeposited CVD films. Pressure = 100 Torr, $x_{CO2} = 0.036$, $x_{MTS} = 0.011$, $x_{AlCl3} = 0.009$, and total flow rate = 250 cm^3/min. a) Temperature = 1000°C, position = 4 cm; b) Temperature = 950°C, position = 7 cm; c) Temperature = 1000°C, position = 7 cm. 19

1. BACKGROUND INFORMATION

Silicon-based ceramic materials are used or being considered for use in a variety of applications related to coal utilization and other energy-related systems. In particular, silicon carbide (SiC), in monolithic or composite form, exhibits such a unique combination of high thermal shock resistance, high thermal conductivity, high strength, low weight, and high oxidation resistance at elevated temperatures that it appears to be the material of choice for a number of technological applications. These include structural components in advanced coal technologies, such as IGCC (integrated gasification combine cycle) and PFBC (pressurized fluidized-combustion) systems, components of advanced turbine systems (combustor liners and, possibly, turbine blades), parts in piston engines (valves and piston heads), ceramic tubes as heat exchangers in coal-fired boilers and industrial furnaces (glass melting and aluminum remelt operations), and ceramic filters for particulate from hot flue and coal gases.

Like Si itself and other Si-based ceramics and intermetallics (silicon nitride and molybdenum disilicide, for instance), the good oxidation resistance of SiC at high temperatures is due to the formation of a scale of SiO_2, through which the oxidizing agent (O_2) must diffuse to reach unreacted material. SiO_2 has one of the lowest diffusion coefficients of O_2 (Jacobson, 1993), and as a result, this passive oxidation process is a slow process. At very high temperatures, formation of gaseous SiO becomes possible, and the oxidation process moves into a phase of active oxidation, where because of absence of a protective scale, the rate of the reaction is very high (Wagner, 1958; Pareek and Shores, 1992; Zheng et al., 1992; Sickafoose and Readey, 1993; Nickel et al., 1993). This pattern of oxidation is qualitatively the same for all Si-based materials, but the location of the passive to active oxidation transition boundary on the [oxygen partial pressure, temperature] plane varies with each material (Jacobson, 1993).

In a typical application, there are several trace components present in the combustion environment in addition to fuel and oxygen. Among the most important ones are alkalis (Na, K), halides (Cl, I), and sulfur (S). All these pollutants are present in relatively large quantities in coal and other solid fuels (waste material, for instance), but even some of the cleanest fuels (such as, unleaded gasoline, commercial aviation fuel, and

fuel oils) contain significant amounts of sulfur (0.05-1%) and alkali compounds (4-20 ppm) (Jacobson, 1993). Sodium and halides may also be introduced in the combustion system through the combustion air, especially if combustion occurs in the vicinity of a marine environment. Corrosive degradation of ceramic components occurs by both gaseous and liquid species formed from the various alkali, halide, and sulfur precursors in the high-temperature environment.

Alkali-induced corrosion through liquid deposition of alkali metal salts and oxide slags is the major mechanism of corrosion. The main corrosive species is Na_2O (or K_2O), formed from sulfites or other salts, which tends to react with the protective scale of SiO_2) forming liquid sodium silicate species ($Na_2O{\cdot}(SiO_2)_x$). In contrast to SiO_2, this liquid layer is not protective because the diffusion coefficient of oxygen in it is much higher than that in SiO_2 and because in the high temperature environment it is carried away from the surface through vaporization. The situation is exacerbated in the presence of moisture since more reactions that lead to formation of Na_2O become thermodynamically more favorable (Van Roode et al., 1993). This corrosion process is not much different from the hot corrosion of turbine alloys that is observed under Na_2SO_4 generating conditions and the corrosion that occurs in SiC heat exchanger tubes when alkali halide fluxes are used in the aluminum remelt industry. Surface recession rates of almost 1 cm/yr may be observed under these circumstances (Goldfarb, 1988; Van Roode et al., 1993).

Given the exceptional properties of SiC and of other silicon-based ceramics but their problematic performance in alkali and sulfur containing environments, a protective coating must be used on surfaces exposed to the combustion environment to protect them from corrosion. For proper performance, such a coating must have good oxidation resistance and chemical stability (up to at least 1300^{o}C), good adherence with the base material, and good tolerance to thermal cycling. Problem-free performance during thermal cycling requires that the chosen material must be such that it yields low residual stress at the interface, and this in turn necessitates that there is a good match between the thermal expansion coefficient of the substrate and that of the coating.

Alumina presents very good corrosion resistance against the various corrosive compounds that cause degradation of the silica scale that functions as a protective layer of

Si-based ceramics (Goldfarb, 1988; Lawson et al., 1993). Under some conditions the presence of Na_2O in the sodium salt melts can lead to formation of a β/β"-alumina (Van Hoek et al., 1991,1992), but, as it is evidenced from the long-term, stable performance of β"-alumina ceramics as electrolytes in Na/S cells, further reaction between the β/β"-alumina and the sulfur and alkali compounds is practically absent (Gordon et al., 1992). Its high corrosion resistance combined with its relatively low cost makes alumina an ideal candidate as protective coating for silicon carbide, but the problem is that its thermal expansion coefficient is almost twice as large as that of the latter.

In such intractable problems such as joining dissimilar materials (metals and ceramics) and depositing adherent and crack-free films and coatings on substrates having significantly different thermal expansion coefficients, compositionally graded materials (CGM's) provide practical solutions (Ford and Stangle, 1993). In graded materials the composition is varied continuously or in steps between those of two outermost layers. The continuous change in the composition and, hence, microstructure of CGM's results in gradients in their properties, and this makes possible to develop coherent structures that present considerably different properties at the two ends of their thickness. Of particular interest for application to protective coatings is the ability of CGM's to bridge the difference in the thermal expansion coefficients of a base layer, which adheres well to the substrate and matches well its thermal expansion coefficient, and of an outer layer, which exhibits the desired properties of chemical stability and corrosion resistance. By spreading the mismatch of the thermal expansion coefficient over a finite thickness, the local thermal stresses – compressive or tensile depending on which thermal expansion coefficient is larger and in which direction the temperature is changed – are reduced and excessive damage to the coating is avoided (Ford and Stangle, 1993).

It is practically impossible to find a single material that matches the thermal expansion coefficient of the substrate material (SiC for our studies), adheres well to the substrate, and exhibits good oxidation resistance in the presence of alkali, sulfur, and halogen compounds. Good oxidation resistance more or less requires that the coating be an oxide, but going through a database of thermal expansion coefficients of oxide ceramics, one soon comes to the realization that there is no oxide that both has thermal

expansion coefficient matching that of SiC over the whole temperature range and provides acceptable protection against oxidation and corrosion. There is relatively good agreement between the thermal expansion coefficient of mullite and SiC, but, even though mullite does not contain free silica, there is some evidence in the literature that it tends to form sodium aluminosilicates and silicates in an alkali and sodium environment (Dietrichs and Krönert, 1982; Van Roode et al., 1993). As we mentioned in the previous section, much better corrosion resistance is displayed by alumina, but its thermal expansion coefficient is almost a factor of 2 greater than that of SiC. The above discussion points to the conclusion that a solution to the problem is offered by a compositionally graded structure, in which the composition varies smoothly between a base layer of mullite, used to provide good adhesion and matching of the thermal expansion coefficient, and an outer layer of alumina, which protects the substrate against corrosion and oxidation.

To reduce the mismatch between alumina and silicon carbide substrates, Federer et al. (1989) and Van Roode et al. (1993) produced graded coatings with composition varied in 25% steps between that of mullite (inner layer) and alumina (outer coating) using a plasma spraying method. Their corrosion tests showed that the mullite-alumina graded structures did very well during thermal cycling, showing no visible damage and developing only a few cracks. However, examination of the substrate-coating interface revealed the presence of sodium aluminosilicates ($Na_2O{\cdot}Al_2O_3{\cdot}SiO_2$) and, possibly, sodium silicates. Their conclusions were that the problem lied in the porosity (10-15%) of the coating produced by plasma spraying and that denser coatings were needed for successful application of the graded coating concept.

The development of processing routes for the fabrication of mullite/alumina graded ceramic coatings through chemical vapor deposition (CVD) methods is the subject of the present research proposal. Silica and alumina will be deposited using mixtures of their chlorides with H_2 and CO_2, and the composition of the deposit will be varied normal to the surface by changing the temperature, pressure, or composition of the gas phase. Experimental deposition studies will be carried out in a hot-wall reactor coupled with a thermogravimetric analysis system, which has already been used successfully in

our laboratory to study SiC deposition from methyltrichlorosilane. Detailed kinetic models of the deposition processes of silica, alumina and mullite will be developed along the general lines of the procedures we used to do so for SiC deposition. These models will be used for data analysis and process scale-up. The deposits will be characterized by a variety of methods (XRD, Raman spectroscopy, electron microscopy, EDX, and electron microprobe analysis) and will be tested for corrosion using various procedures.

2. WORK DONE AND DISCUSSION

During this reporting period, we continued the experimental work on the investigation of the codeposition of alumina, silica, and aluminosilicates from mixtures of methyltrichlorosilane (MTS), aluminum trichloride, carbon dioxide, and hydrogen and the deposition of the simple oxides, alumina and silica, from mixtures containing only one chloride ($AlCl_3$ and MTS, respectively). Experiments were carried out to investigate the effects of the composition of the gas phase mixture and the residence time of the mixture in the reactor for temperatures in the range 800-1000^{o}C, 100 Torr pressure, 0.006-0.015 $AlCl_3$ feed mole fraction, 0.011-0.027 CH_3SiCl_3 feed mole fraction, and 0.004-0.07 CO_2 feed mole fraction, and various positions along the axis of the deposition reactor. Some of the obtained results are presented and discussed below.

Results on the influence of the feed composition on the deposition rates are presented in Figures 1-4. The effects of CO_2 mole fraction at 950 and 1000^{o}C are presented in Figures 1 and 2, respectively, for mole fraction variations in the range 0.004-0.07 at 950^{o}C and 0.02-0.07 at 1000^{o}C, with all the other reactants concentrations kept constant (0.011 MTS mole fraction and 0.009 $AlCl_3$ mole fraction). From the results shown in these figures, one concludes that an increase in the mole fraction of CO_2 has a positive effect on the reaction rate of the codeposition process at both temperatures. A steep increase in the deposition rate is observed with increasing mole fraction for low mole fraction values and there is a tendency for the rate to reach a “plateau” value at higher concentrations (Figure 1). This effect is more clear in the results obtained at 950^{o}C, whereas at 1000^{o}C, the codeposition rate appears to go through another increasing phase at the upper range of CO_2 mole fraction. In Figure 1, the codeposition rate vs. CO_2

mole fraction data are shown for two experimental runs, and it is seen that the experimental results are characterized by very good reproducibility.

Since the total flow rate remains constant at 250 cm^3/min, the increase of the CO_2 feed mole fraction is accompanied by a decrease in the H_2 mole fraction in the feed. However, since the mole fraction of H_2 is very large, this decrease is relatively small, and therefore it cannot account for the leveling off of the codeposition rate as the CO_2 mole fraction is increased. The thermodynamic equilibrium computations showed that the increase in the mole fraction of CO_2 in the feed leads to a marked increase in the equilibrium concentration of H_2O, but at the same time, it reduces considerably the concentrations of the various metal chlorides species, especially those of silicon chlorides. This is due to the increase in the concentrations of the oxygen-containing species, because of the higher amounts of oxygen available in the mixture. These results suggest that the leveling off of the deposition rate at high concentrations of CO_2 is the result of the competition of the increasing concentration of H_2O and the decreasing concentrations of metal chlorides.

In the case of silica deposition, the results in the variation of the deposition rate show that the increase in the mole fraction of CO_2 has, in general, a negative effect in the deposition rate of silica, with the only exception being at very low CO_2 mole fractions (0.004-0.008) and 950^oC (Figure 1). Apparently, the decrease in the concentrations of silicon chlorides with the increase in the CO_2 mole fraction has a much stronger effect on the deposition rate than the increase in the concentration of H_2O, for moderate CO_2 mole fractions. The variation of the deposition rate of alumina exhibits the same behavior as that of the codeposition rate (Figures 1 and 2). This suggests that the surface reaction steps that are responsible for the enhanced deposition of silica in the codeposition process are affected by the concentration of CO_2 in a similar manner as the steps leading to the SiO_2 deposition in the single species deposition process. The deposition rate of alumina appears to level off at lower CO_2 mole fraction values than the codeposition rate, and this happens at higher CO_2 mole fractions as the temperature increases. These trends are consistent with previous experimental studies on Al_2O_3 CVD from $AlCl_3$-CO_2-H_2 mixtures (Colmet et al., 1982; Kim et al., 1982; Park et al., 1983) where both a maximum

in the alumina deposition rate and a shift of the location of the maximum with the temperature were observed. These results led to conclude the limiting mechanism in alumina CVD was the water gas-shift reaction. The production of water vapor from CO_2 and H_2 has been also suggested by Wong and Robinson (1970) to be the rate-limiting step in the deposition of Al_2O_3. Funk et al. (1976) found that the increase of CO_2 flow rate had a positive effect on the deposition rate of alumina, but they did not examine the possibility of the occurrence of a maximum.

More results on the influence of the feed composition on the deposition rates are shown in Figure 3 which presents the variation of the deposition rate with the $AlCl_3$ mole fraction in the presence or absence of MTS at 950 and 1000^oC, respectively. The $AlCl_3$ mole fraction varied in the range 0.006-0.015, and this corresponded to a range of 0.55-1.36 Al/Si feed ratio. The feed content in the other reactants was 0.036 CO_2 mole fraction and 0.011 MTS mole fraction, whereas the distance of the midpoint of the substrate from the top of the heating zone was 4 cm. It is seen that an increase of the $AlCl_3$ flow rate (via an increase in the flow rate of HCl sent through the chlorinator) leads to an increase in the rates of both deposition processes, and this effect intensifies with increasing temperature. As before, the rate of the codeposition is much higher than that of Al_2O_3 deposition. The results of past experimental studies on the chemical vapor deposition of alumina (Colmet and Naslain, 1982; Colmet et al., 1982; Kim et al., 1982; Park et al., 1983) are in good agreement with those of the present study. Colmet et al. (1982) reported that at low $AlCl_3$ concentrations (close to the values employed in this investigation), the deposition rate first rapidly increased with increasing $AlCl_3$ mole fraction, and then approached a limiting value. This was interpreted as an indication that the deposition rate of alumina was limited by mass transport in the gas phase. A trend to reach a limiting value is not observed in Figure 3, but this could be a result of the different reactor configuration and flow rates used in our experiments.

Kim et al. (1982) found a maximum in the deposition rate for $AlCl_3$ mole fractions in the 0.01-0.015 range. It was suggested that the decrease in the deposition rate at higher $AlCl_3$ mole fractions may be caused by the increased concentration of HCl in the gas phase. In an effort to identify the cause of this decrease, Funk et al. (1976)

investigated the effect of HCl on the deposition rate of alumina, and found that addition of HCl to the feed mixture decreased the deposition rate. Since the increase of the mole fraction of $AlCl_3$ is not accompanied by an increase in the mole fraction of CO_2, the weakening influence of $AlCl_3$ on the deposition rate of alumina and the codeposition rate could be due to the overall process becoming controlled by the supply of water through the water gas-shift reaction. According to Silvestri et al. (1978), the dependence of the deposition rate of Al_2O_3 on both the $AlCl_3$ and CO_2 mole fractions is an indication that the process involves more than one rate-limiting steps.

Figure 4 presents the effect of the MTS mole fraction on the deposition rate of SiO_2 at 950^{o}C, 100 Torr, 250 cm^3/min total flow rate, 0.036 CO_2 mole fraction, and two locations of the midpoint of the substrate, 4 cm and 7 cm from the top of the heating zone of the furnace. When the substrate is positioned at 7 cm, an increase in the MTS mole fraction leads to an increase in the deposition rate, but the opposite behavior is observed at 4 cm. The rate of silica deposition increases with increasing distance from the top of the heating zone except for very low MTS mole fractions. Since low chloride mole fractions (around 0.01) are usually employed in our experiments, this result indicates that in order to obtain significant deposition rates the substrate should not be placed far from the top of the heating zone of the reactor.

Results on the effect of the substrate position in the reactor on the deposition rate of Al_2O_3 and the codeposition at 950 and 1000^{o}C with 0.009 $AlCl_3$ mole fraction, 0.011 MTS mole fraction, and 0.036 CO_2 mole fraction, can be extracted by comparing Figures 1 and 3, and 2 and 3, respectively. At 950^{o}C, an increase in the distance from the top of the heating zone leads to lower deposition rates. Specifically, the rate of Al_2O_3 deposition is 0.0077 mg/cm^2·min at 4 cm, and 0.0056 mg/cm^2·min at 7 cm, whereas the codeposition rate is 0.024 mg/cm^2·min at 4 cm, and 0.022 mg/cm^2·min at 7 cm. On the other hand, at 1000^{o}C there is an increase in the rate of both reactions as the distance goes from 4 to 7 cm! The rate of alumina deposition increases from 0.0135 to 0.016 mg/cm^2·min, and that of codeposition from 0.049 to 0.068 mg/cm^2·min. The location of the substrate also affected the composition of the deposit (see data presented in last report). These results lead to the conclusion that the role of the substrate location must be taken under

consideration when selecting operating conditions for deposition of aluminosilicates since it directly affects the residence time of the reactant molecules in the hot zone of the reactor upstream of the substrate. A detailed investigation of the dependence of the deposition rate on the position in the reactor is intended to be carried out in the future.

The composition and morphology of the deposits were determined using energy dispersive X-ray analysis (EDXA) and scanning electron microscopy (SEM), respectively. Figures 5 and 6 show some representative SEM micrographs of silica, alumina, and codeposited films obtained at 100 Torr, 250 cm^3/min total flow rate, 0.011 MTS mole fraction, 0.009 $AlCl_3$ mole fraction, and a CO_2 mole fraction of 0.036 at various locations and temperatures. The thickness of the films varied between 5 and 12 μm. The characterization of the silica deposits revealed that they consisted of amorphous SiO_2, and their photomicrographic examination by electron microscopy showed that they were smooth and dense, having globular morphology with average globule size of approximately 13 μm (Figure 5a). On the other hand, the alumina films were characterized by much larger globule sizes, up to about 30 μm (Figure 5b). X-ray diffraction (XRD) showed that alumina coatings consisted primarily of polycrystalline κ-Al_2O_3, but incorporation of the θ modification was also encountered. Annealing of the coatings in an inert atmosphere at 1400°C resulted in transformation of κ-Al_2O_3 to θ-Al_2O_3 (corundum).

The growth of θ-Al_2O_3 is often initiated by the κ- → θ-Al_2O_3 transformation during the deposition process (Fredriksson and Carlsson, 1989, 1993) and κ-Al_2O_3 is the phase grown initially irrespective of the CVD process temperature. An increase in the deposition time leads to increased θ/κ ratio. It has been reported that the appearance of the θ-phase depends on the deposition temperature, occurring earlier at higher temperatures. Specifically, it has been found that deposition for 5 hr at 960°C gave XRD peaks of θ-Al_2O_3 in the deposit with very weak intensities, whereas 15 min of deposition time at 1080°C was ample to yield deposit with intense θ-Al_2O_3 diffraction peaks (Fredriksson and Carlsson, 1989). This observation agrees with our results since our the alumina samples were prepared at temperatures up to 1000°C, and the overall deposition time varied between 60 and 85 min.

The films deposited from MTS-$AlCl_3$-CO_2-H_2 mixtures were found to be smooth, dense, and uniform in thickness, having globular structure (Figure 6a) similar to that of the alumina films. The size of the globules in the codeposits tended to increase with increasing temperature; an average globule size of about 20 μm was observed at 950°C, while at 1000°C the deposit consisted of globules of about 35 μm. In some cases, in which the supply of MTS to the reactor was stopped before that of $AlCl_3$, small alumina crystals were found to exist on the external surface of the coating (see Figure 6b). This result lends further support to the conclusion that the presence of decomposition products of MTS in the gas phase suppresses the deposition of alumina. Formation of cracks, possibly induced by contact stresses, was observed in some of the samples. Figure 6c shows some cracks formed in a film prepared at 7 cm into the heating zone at 1000°C and 100 Torr. Alumina flakes are also seen to exist on the surface of this film as well.

Several codeposited films were analyzed with XRD, but in all cases they were found to be amorphous (no crystalline phase was detected). The elemental composition of the deposits was determined by EDXA. Silicon, aluminum, and oxygen were the only elements detected within the sensitivity limits of the analysis, and their relative amounts were consistent with those corresponding to the stoichiometry of mixtures of SiO_2 and Al_2O_3. As we have already pointed out in previous reports, the film composition data showed that the enhancement in the rate of deposition of the codeposition process was due to a dramatic rise in the rate of the deposition of SiO_2, accompanied by a reduction in the rate of Al_2O_3 deposition. Therefore, the results of the kinetic investigation of the individual deposition processes of silica and alumina cannot be used for the derivation of conclusions about the behavior of the codeposition process. The latter must be studied independently in order to be sufficiently characterized, and, in order to identify the region of operating parameters where deposition of films of a certain Al_2O_3/SiO_2 ratio can be achieved.

3. **SUMMARY**

The deposition of silica, alumina, and aluminosilicate species from MTS-H_2-CO_2, $AlCl_3$-H_2-CO_2, and MTS-$AlCl_3$-H_2-CO_2 mixtures was investigated at subambient

pressures (100 Torr) in a gravimetric hot-wall reactor coupled with an electronic microbalance. The experimental conditions covered broad ranges of temperature (800-1100^{o}C), and gas-phase composition (0.004-0.07 CO_2 mole fraction, 0.006-0.015 $AlCl_3$ mole fraction, 0.011-0.027 MTS mole fraction). The morphology, composition, and microstructure of the films were determined employing SEM, EDXA, and XRD. Amorphous silicon oxide and codeposited films were obtained, while κ-Al_2O_3 was the main deposition product in the aluminum oxide coatings. The behavior of the experimental results was discussed in the context of thermodynamic equilibrium calculations for the feed compositions used in the experiments.

The mole fraction of CO_2 had a strong influence on the deposition rates of all three processes. The alumina deposition and codeposition rates increased with increasing the concentration of CO_2 in the feed, and in both cases they tended to reach a plateau. The increase in the concentration of carbon dioxide had, in general, a negative effect on the rate of silica deposition. The thermodynamic analysis results suggested that the above effects could be due to the fact that an increase in the concentration of CO_2 in the feed leads to higher concentration of H_2O at equilibrium, but, at the same time, decreases the concentrations of metal chlorides, especially those of silicon. The increase in the mole fraction of $AlCl_3$ had a positive effect on the rate of codeposition and the deposition of alumina. In the case of alumina deposition, the deposition rate tended to level off, in some cases, with increasing $AlCl_3$ concentration, and this behavior was consistent with the results of past experimental studies on the chemical vapor deposition of Al_2O_3. The deposition rate and the deposit stoichiometry were influenced strongly by the substrate position in the reactor, and the deposition rate could increase or decrease with increasing distance from the entrance of the reactor depending on the reaction temperature. A comprehensive study of the influence of the substrate location on the deposition rate and the deposit stoichiometry is among our future research plans.

BIBLIOGRAPHY

Dietrichs, P., Krönert, W., INTERCERAM·NR. 3, 223 (1982).

Colmet, R., Naslain, R., Wear, 80, 221 (1982).

Colmet, R., Naslain, R., Hagenmuller, P., Bernard, C., J. Electrochem. Soc., 129, 1367 (1982).

Ford, R.G., Stangle, G.C., Proc. 6th Conf. Cer. Matrix Comp., p. 795 (1993).

Federer, J.I., Van Roode, M., Price, J.R., Surface and Coatings Technology, 39/40, 71 (1989).

Fredriksson, E., Carlsson, J.-O., J. Phys., 50 (C-5), 391 (1989).

Fredriksson, E., Carlsson, J. -O., Surf. Coat. Tech., 56 (2), 165 (1993).

Funk, R., Schachner, H., Triquet, C., Kornmann, M., Lux, B., J. Electrochem. Soc., 123 (2), 285 (1976).

Goldfarb, V., GRI Contract No. 5086-232-1274, Final Report (1988).

Gordon, R.S., Heavens, S.N., Virkar, A.V., Weber, N., Corrosion Science, 33, 605 (1992).

Jacobson, N.S., J. Amer. Cer. Soc., 76, 3 (1993).

Kim, J. G, Park, C. S., Chun, J. S., Thin Solid Films, 97 (1), 97 (1982).

Lawson, M.G., Pettit, F.S., Blachere, J.R., J. Mater. Res., 8, 1964 (1993).

Nickel, K.G., Fu, Z., Quirmbach, P., Trans. ASME, 115, 76 (1993).

Pareek, V.K., Shores, D.A., Science, 48, 983 (1992).

Park, C. S., Kim, J. G., Chun, J.S., J. Vac. Sci. Technol. A, 1 (4), 1820 (1983).

Sickafoose, R.R., Jr., Readey, D.W., J. Am. Cer. Soc., 76, 316 (1993).

Silvestri, V. J., Osburn, C. M., Ormond, D. W., J. Electrochem. Soc., 125 (6), 902 (1978).

Van Hoek, J.A.M., van Loo, F.J.J., Metselaar, R., Key Eng. Materials, 53-55, 111 (1991).

Van Hoek, J.A.M., van Loo, F.J.J., Metselaar, R., J. Am. Cer. Soc., 75, 109 (1992).

Van Roode, M., Price, J.R., Stala, C., J. Eng. Gas Turb. Power, 115, 139 (1993).

Wagner, C., J. Appl. Physics, 29, 1295 (1958).

Wong, P., Robinson, McD., J. Amer. Cer. Soc., 53 (11), 617 (1970).

Zheng, Z., Tressler, R.E., Spear, K.E., Corrosion Science, 33, 545 (1992).

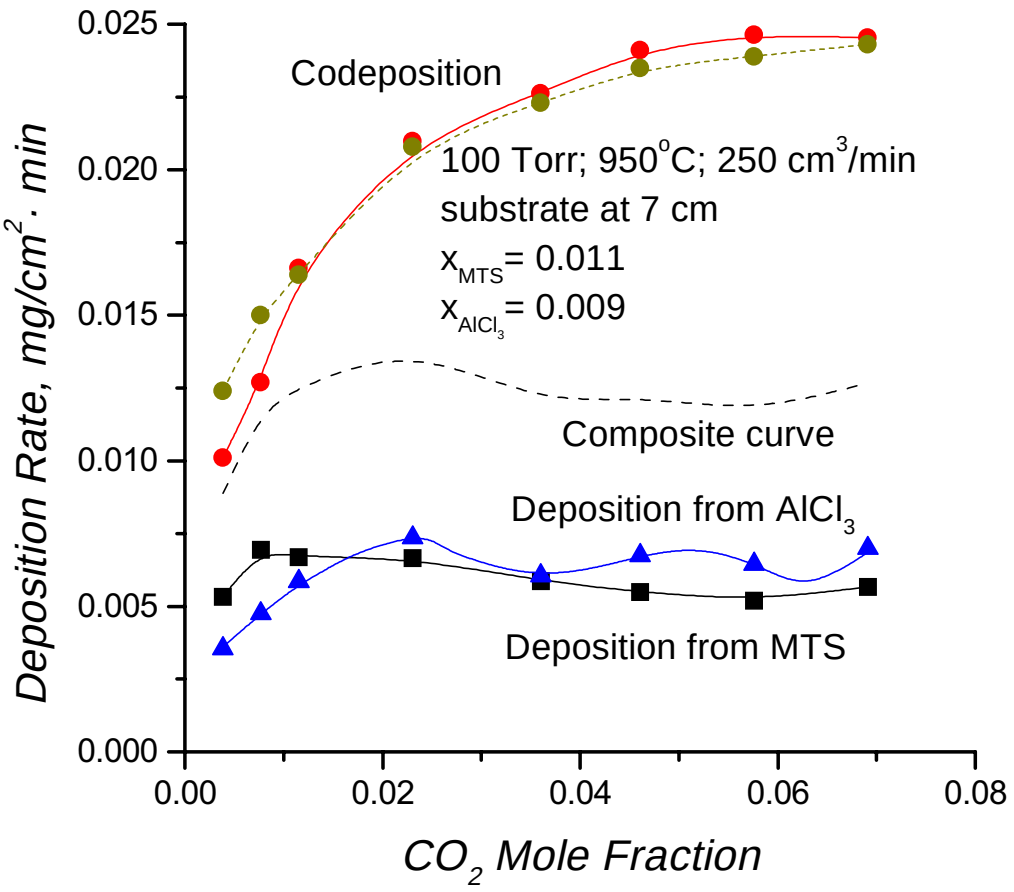

Figure 1. Effect of CO_2 mole fraction on the deposition and codeposition rates at 950°C.

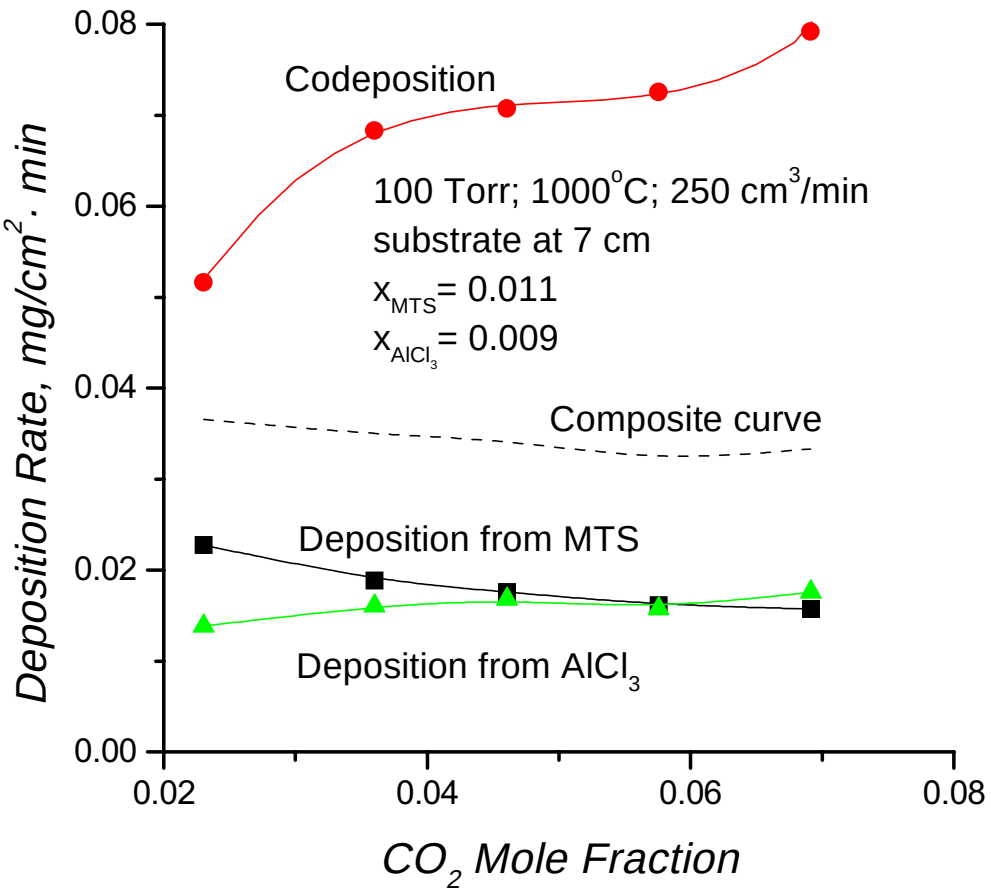

Figure 2. Effect of CO_2 mole fraction on the deposition and codeposition rates at 1000°C.

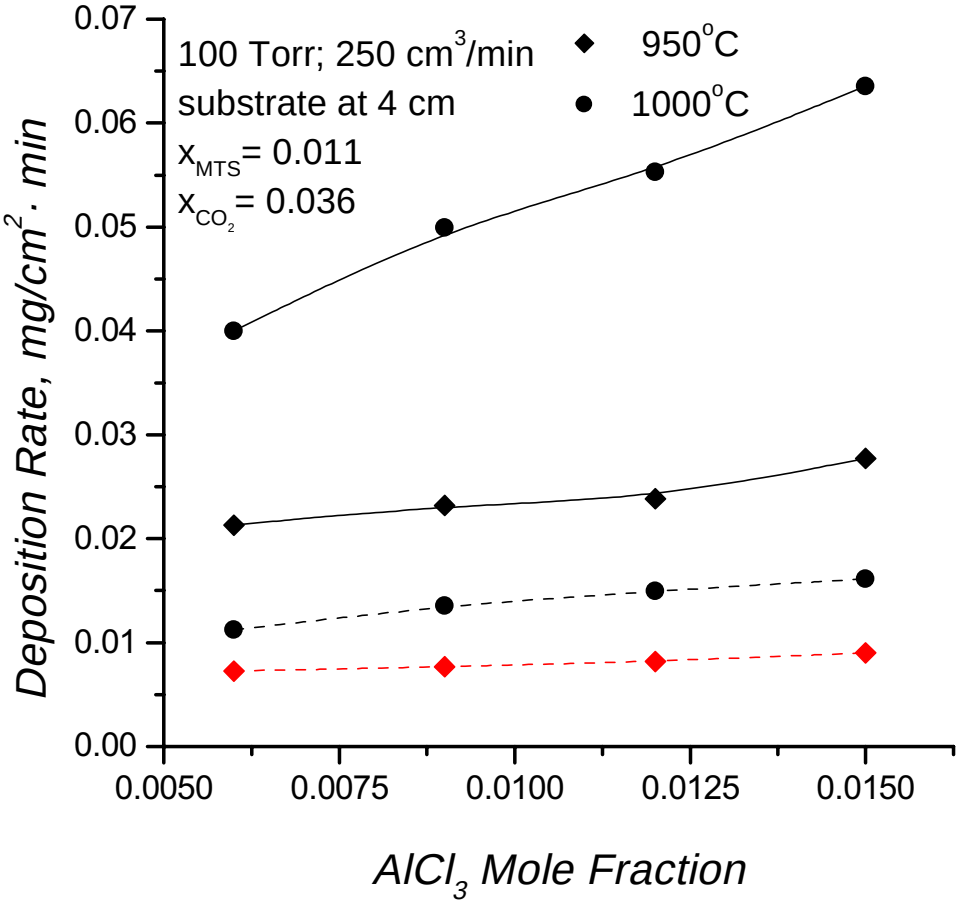

Figure 3. Effect of $AlCl_3$ mole fraction on the deposition rate in the presence or absence of MTS at 950°C and 1000°C. Solid lines: codeposition; dashed lines: deposition from $AlCl_3$.

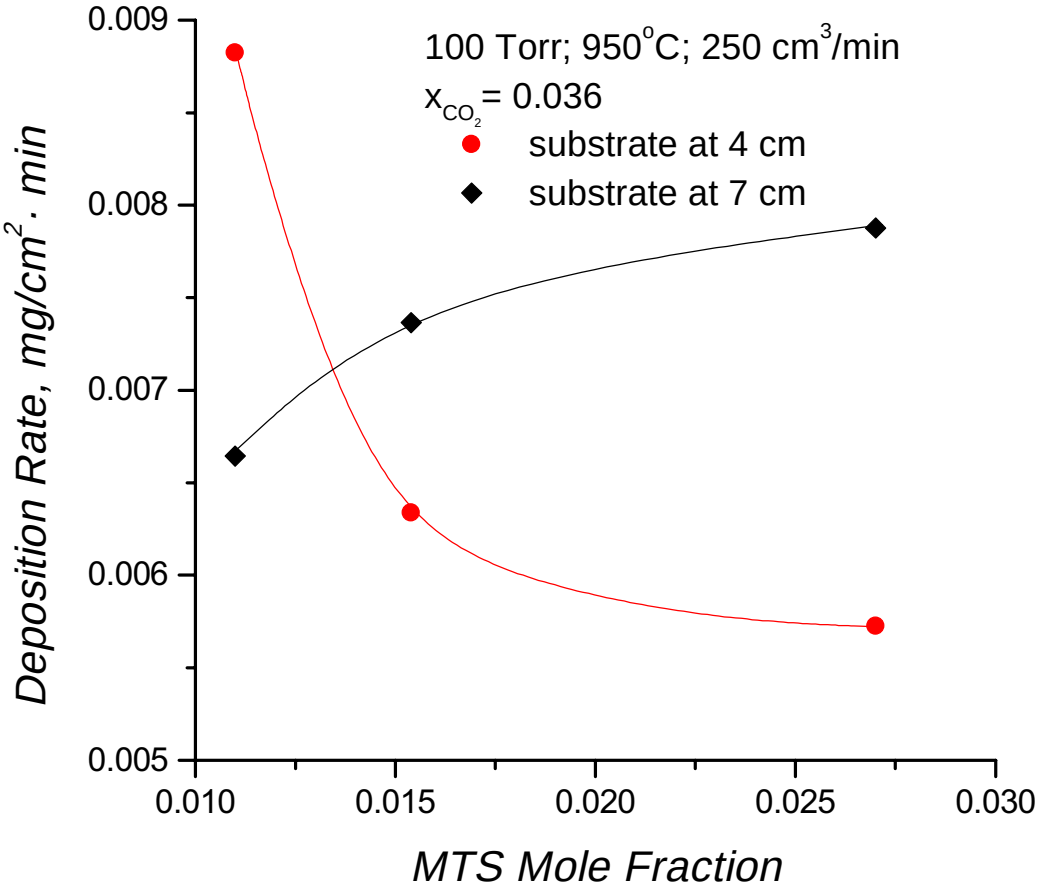

Figure 4. Effect of MTS mole fraction on the rate of SiO_2 deposition at 950 ^{o}C.

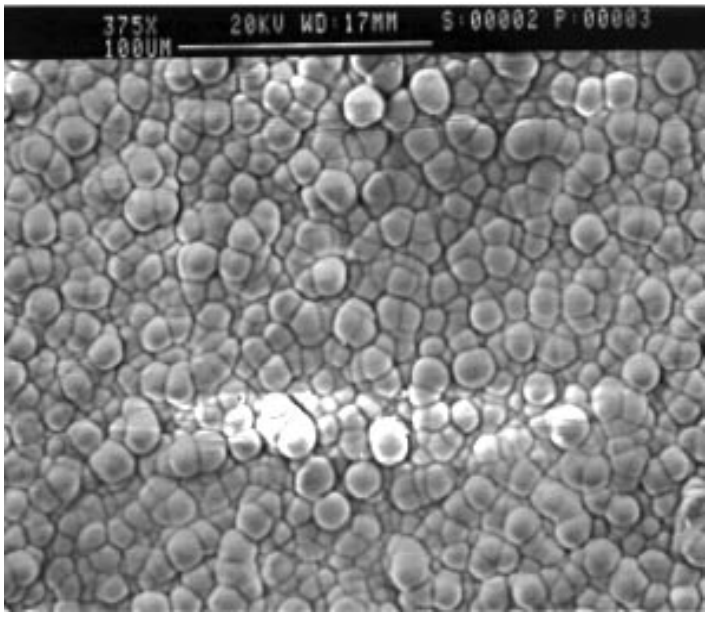

(a)

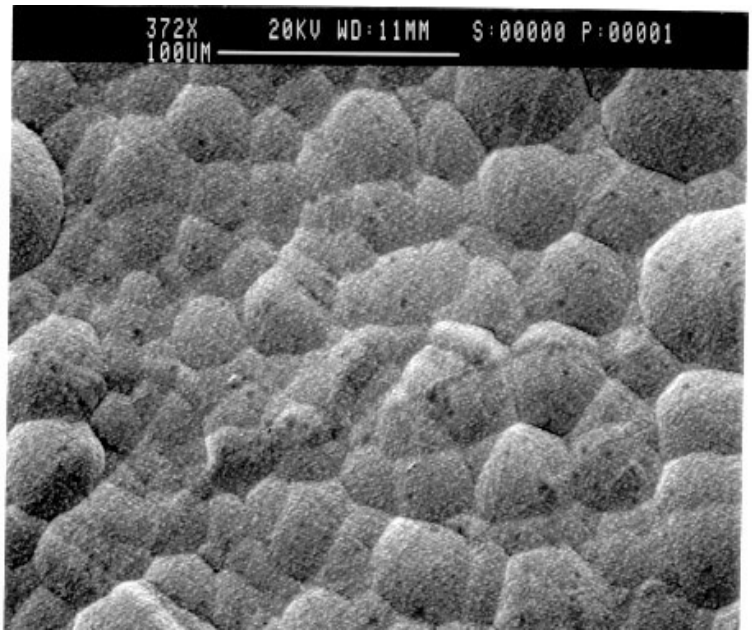

(b)

Figure 5. SEM micrographs of CVD films. Temperature = 1000^{o}C, pressure = 100 Torr, x_{CO2} = 0.036, total flow rate = 250 cm^{3}/min, and position = 4 cm. a) silica, x_{MTS} = 0.011; b) alumina, x_{AlCl3} = 0.009.

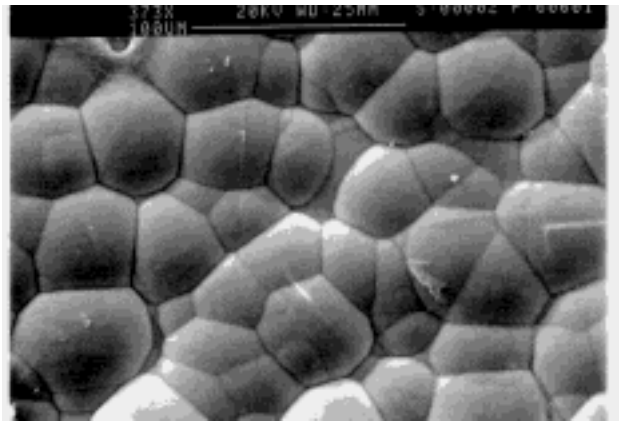

(a)

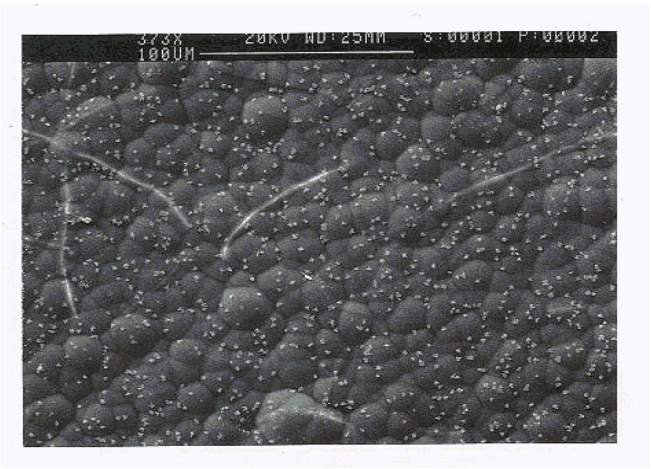

(b)

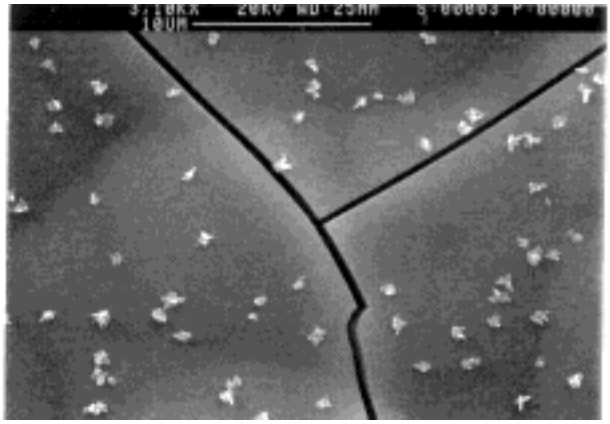

(c)

Figure 6. SEM micrographs of codeposited CVD films. Pressure = 100 Torr, x_{CO2} = 0.036, x_{MTS} = 0.011, x_{AlCl3} = 0.009, and total flow rate = 250 cm^3/min. a) Temperature = 1000^{o}C, position = 4 cm; b) Temperature = 950^{o}C, position = 7 cm; c) Temperature = 1000^{o}C, position = 7 cm.